Available online at www.sciencedirect.com
SCIENCE DIRECT
Catalysis Today 106 (2005) 149–153
CATALYSIS TODAY
www.elsevier.com/locate/cattod

Novel utilization of MCM-22 molecular sieves as supports of cobalt catalysts in the Fischer–Tropsch synthesis

Raman Ravishankar, Mianhui M. Li, Armando Borgna *

Institute of Chemical and Engineering Sciences, 1 Pesek Road, Jurong Island 627833, Singapore

Abstract

Cobalt catalysts (2–10 wt% Co) supported on silica-rich MCM-22 zeolites have been prepared by impregnation with aqueous $Co(NO_3)_2$ solutions. The catalysts are characterized by X-ray fluorescence (XRF), X-ray diffraction (XRD), nitrogen adsorption, solid state nuclear magnetic resonance (NMR), scanning electron microscopy (SEM), high-resolution transmission electron microscopy (TEM) and X-ray photoelectron spectroscopy (XPS). The catalytic properties for the Fischer–Tropsch synthesis (FTS) at 280 °C, 12.5 bar and $H_2/CO = 2$ are evaluated. The catalysts supported on MCM-22 exhibit the highest selectivity to long-chain (C_{5+}) hydrocarbons when MCM-22 supports are synthesized with the appropriate Si/Al ratio.

Keywords: MCM-22 molecular sieves; Cobalt catalysts; Fischer–Tropsch synthesis

1. Introduction

In recent years, the conversion of natural gas to liquids (GTL) via the Fischer–Tropsch synthesis (FTS) process has received renewed interest mainly due to the vast reserves of natural gas, the need to monetize remote or stranded natural gas, the decreasing quality of crude oils, the tighter fuel specifications and the excellent quality of the synthetic FT fuels. Nowadays, the Fischer–Tropsch process is an attractive route to produce clean fuels, chemicals and other value-added products [1,2].

Cobalt-supported catalysts are currently preferred over Fe-based systems due to their superior performance, since they favor the formation of long-chain *n*-paraffins, are more stable against deactivation by water and are less active in water gas-shift (WGS) reaction [3,4]. Typically, Co-FTS catalysts consist of small metallic Co particles supported onto amorphous oxide carriers such as SiO_2, Al_2O_3 or TiO_2. Although it has been reported that the support might play an important role in determining the product distribution, the effect of the support and its porosity remains still unclear [5]. The development of effective catalysts with controlled product selectivity is a difficult task and remains one of the biggest challenges [6].

Recently, microporous and mesoporous molecular sieves were used as supports for preparing Co-based FTS catalysts, aiming the improvement of the FT activity and selectivity by confining the metal particles inside the channels [7]. These ordered materials might provide the required geometric constraints to control the product distributions successfully. Most of these studies have been restricted to conventional microporous materials like ZSM-5, zeolite Y, mordenite and a mesoporous molecular sieve, MCM-41. Thus, the use of new micro- and mesoporous materials with controlled acid–base properties might be the key to control the FT selectivity.

MCM-22 molecular sieve (MWW structure) is distinguished by an unusual structure, consisting of layers linked together along the *c*-axis by oxygen bridges and containing two independent pore systems. In addition, its typical thin platelet morphology results in high external surface area [8,9]. Therefore, in this contribution, we report on the use of MCM-22 molecular sieves with different Si/Al ratios as supports for preparing cobalt-based Fischer–Tropsch catalysts.

* Corresponding author. Tel.: +65 67963802; fax: +65 63166182.
E-mail address: armando_borgna@ices.a-star.edu.sg (A. Borgna).

0920-5861/$ – see front matter © 2005 Elsevier B.V. All rights reserved.
doi:10.1016/j.cattod.2005.07.123

2. Experimental

2.1. Catalyst preparation

The hydrothermal synthesis of the layered aluminosilicate MCM-22 (P) was carried out by using hexamethyleneimine as organic template under static conditions. Typically, 0.3 g of anhydrous sodium aluminate (Riedel de Haën, Al_2O_3 50–56%, Na_2O 40–45%) and 0.9 g of sodium hydroxide (Merck) were dissolved in 112 g deionized water. The solution was stirred well for 15 min. 6.6 g of hexamethyleneimine (Fluka, >97%) was added dropwise under vigorous stirring. The mixture was left undisturbed for 1 h. 7.9 g fumed silica (Aldrich, 99.8%, 0.07 μm) was added in portions to the stirring mixture and the resulting slurry was stirred vigorously. The resulting slurry was stirred well for 1 h, loaded in Teflon-lined SS autoclaves and heated under static conditions at 150 °C for 12 days. Finally, the sample was filtered, washed thoroughly with deionized water and dried at 85 °C for 1 h. MCM-22 zeolites were obtained by the calcination of MCM-22(P) precursors at 550 °C during 8 h in a muffle furnace. The variation in the Si/Al ratios was achieved by varying the amounts of fumed silica. Incorporation of Co was carried out by impregnation of the parent MCM-22 supports with aqueous solution containing the required amount of $Co(NO_3)_2{\cdot}6H_2O$ to achieve the desired nominal concentrations. In order to facilitate Co reduction, the catalysts were promoted with Pt. In all cases, a small amount of Pt (0.1–0.2%) was introduced by co-impregnation using H_2PtCl_6 as precursor. After stirring for 2 h at room temperature, the solvent was eliminated by rotavaporation at 60 °C under vacuum. The solid was further dried overnight at 110 °C. Finally, all Co-supported catalysts were calcined in a muffle furnace at 400 °C for 10 h.

2.2. Catalysts characterization

Elemental analyses were performed by X-ray fluorescence (XRF) in a Bruker S4 Explorer Spectrometer operating in ''Standardless'' mode with full element coverage (Fast-Vac. method). X-ray diffraction (XRD) was used to identify and characterize the nature of the crystalline phases. XRD patterns were obtained at room temperature in a D8 Advance Bruker diffractometer using Cu Kα radiation at 40 kV and 40 mA. Textural properties of the supports and Co-containing catalysts were obtained from the nitrogen adsorption isotherms at −196 °C in a Quantachrome Autosorb-6 equipment. Prior to adsorption measurements, the samples were outgassed at 200 °C for 24 h. The catalysts were further characterized by solid state nuclear magnetic resonance (NMR), scanning electron microscopy (SEM), high-resolution transmission electron microscopy (TEM) and X-ray photoelectron spectroscopy (XPS). ^{29}Si and ^{27}Al solid state NMR spectra were obtained using MAS spinning technique in a 400 MHz Bruker system. Tetramethylsilane (TMS) and aluminum nitrate were used as standards for ^{29}Si and ^{27}Al NMR measurements. The zeolite samples were sputtered with platinum and scanning electron micrographs were recorded using JEOL FESEM JSM-6700F with 2 kV and 10 μA. HRTEM experiments were conducted on a TECNAI TF20 SuperTwin microscope operating at 200 kV. XPS spectra were measured on a VG Escalab 250 spectrometer equipped with an aluminum anode (Al Kα = 1486.6 eV). Measurements were carried out with 20 eV pass energy, 0.1 eV step and 0.1 s dwelling time. Energy correction was performed using the Si 2p peak of SiO_2 at 103.3 eV as a reference.

2.3. Catalytic measurements

The FTS reaction was performed in a fixed-bed stainless-steel reactor (length 30 cm, 15 mm i.d.). Typically, the reactor was loaded with 0.8 g of catalyst (0.21–0.40 mm particle size). Prior to catalytic experiments, the catalysts were reduced in situ overnight at atmospheric pressure under flowing hydrogen (50 ml/min) at 500 °C. After reduction, the reactor temperature was lowered to the reaction temperature and the pressure increased up to 12.5 bar. The samples were analyzed using online Agilent GC6890N fitted with HP-PONA capillary (50 m, 0.2 μm) connected to FID for the analyses of hydrocarbons and Poropak-Q (Supelco) connected to TCD for the analysis of permanent gases. The products were confirmed by Agilent GC–MS 5973.

3. Results and discussion

FT selectivity depends on the presence of acid sites mainly due to the fact that they are able to promote side reactions such as hydrocracking, isomerization and coking [10]. Since it has been reported that the acidity of MCM-22 zeolites decreases as the Si/Al ratio is increased [11], Na-form of MCM-22 zeolites with high Si/Al ratios were synthesized as previously described. Typically, samples with Si/Al ratios between 45 and 200 were synthesized. XRF reveals that Si/Al ratios are slightly higher than those used in the starting gels (theoretical ratios). Fig. 1 displays the XRD patterns of the MCM-22(P) obtained with a Si/Al gel ratio of 45 and the resulting MCM-22 zeolite, samples MCM-22(P)[45] and MCM-22[45], respectively, synthesized under static conditions. The intercalation of hexamethyleneimine between the layers of the MCM-22(P) precursor leads to XRD peaks at $2\theta = 3–5^\circ$, showing the layered morphology of MCM-22(P). Although a single peak in the 3–5° range is usually observed, the XRD pattern of the MCM-22(P) is in good agreement with those reported in the literature [12,13]. The additional peak might point out the presence of layers of varying distances as these peaks characterize the distance between layers. Upon calcination, the layered structure disappears and a well crystallized structure is obtained. Except for the small feature

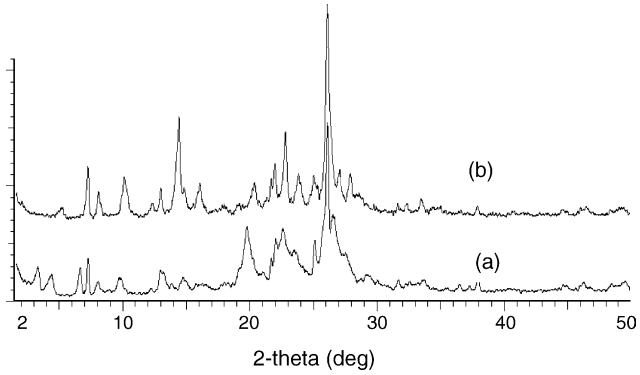

Fig. 1. Powder X-ray diffraction patterns of sample with Si/Al = 45: (a) as-synthesized, MCM-22(P)[45] and (b) calcined, MCM-22[45].

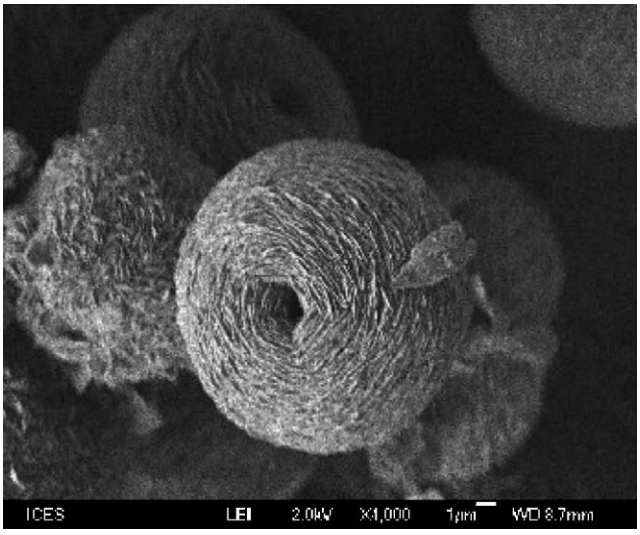

Fig. 2. Scanning electron micrograph of MCM-22(P)[45] sample. Si/Al = 45.

at about 4.5°, all XRD reflections match very well with those of the MCM-22 zeolite [12,13]. The small feature at 4.5° might indicate the formation of a small fraction of a layered silicate structure, which has been observed by other authors [14]. Similar XRD patterns were obtained for other Si/Al ratios. Regardless of the Si/Al ratio, BET surface areas between 350 m^2/g and 400 m^2/g are obtained for the parent MCM-22 zeolites. Zeolite MCM-22[45] exhibits an external surface area, estimated using the *t*-plot method, of 130 m^2/g and a total surface area of 380 m^2/g. Therefore, approximately 35% of the specific surface area can be attributed to the external surface area. Similar values were also obtained for other Si/Al ratios. The total pore volume of the parent MCM-22 zeolites is close to 0.25 cm^3/g, and the micropore volume estimated using the *t*-plot method is between 0.08 cm^3/g and 0.1 cm^3/g.

Fig. 2 shows a typical SEM image of a MCM-22(P) precursor. Large micrometer-sized (∼100–500 μm) spheroidal aggregates of nanoplates (<50 nm) were observed. Upon calcination, cracks were developed due to the elimination of the templates and the stacking of nanoplates was observed (figure not shown). Surface impurities were not observed. Identical morphologies were observed for the samples with different Si/Al ratios. In summary, the synthesis of MCM-22 zeolites with different Si/Al ratios was successfully achieved.

Cobalt-supported MCM-22 zeolites with varying Co loadings were prepared as previously described. XRD measurements indicate that, upon Co impregnation, the MCM-22 structure is still observed. X-ray diffractograms of oxidized Co catalysts with higher metal loadings also exhibit the characteristic reflection of Co_3O_4 phase at $2\theta = 36.9°$, as usually reported for siliceous materials impregnated with cobalt nitrate [5,15]. The ^{29}Si and ^{27}Al solid state NMR spectra reveal no significant changes upon impregnation with Co. Particularly, no extra-framework aluminum was observed after Co-impregnation and subsequent calcination. Table 1 summarizes the main characteristics of Co catalysts supported on MCM-22 molecular sieves. A conventional silica-supported catalyst has also been included as a reference. The Si/Al ratios of the Co catalysts are essentially the same as compared to those obtained for the parent zeolites. Except for Co10/MCM-22[45], the Na/Al ratio is ≥ 1 suggesting that the negative charge in the Al tetrahedrons is compensated by Na cations. In order to investigate the effect of acid sites on the catalytic behavior, the parent zeolite MCM-22[45] was partially exchanged with NH_4NO_3 before the impregnation with Co. The presence of H^+ is indicated by the Na/Al ratio lower than 1. Significant decrease of both surface area and pore volume is observed for all catalysts. This decrease of surface area could be

Table 1
Summary of the different Co catalysts used in FT reaction; chemical composition and textural properties

Sample	Si/Al	Na/Al	Co (%)	Pt (%)	Sg BET (m^2/g)	TPV[a] (cm^3/g)	μPV[b] (cm^3/g)	APD[c] BJH (nm)
Co10/MCM-22[45]	60	0.6	8.5	0.23	206	0.12	0.060	3.1
Co10/MCM-22[90]	129	1.4	8.8	0.20	100	0.10	0.016	3.6
Co10/MCM-22[200]	230	1.4	8.7	0.19	155	0.15	0.010	3.4
Co5/MCM-22[200]	236	1.2	4.6	0.20	145	0.14	0.010	4.8
Co2/MCM-22[200]	220	1.4	2.0	<0.1	135	0.15	0.018	4.4
Co10/SiO_2	–	–	9.8	0.23	360	0.25	0.0	4.0

[a] TPV: total pore volume.
[b] μPV: micropore volume.
[c] APD: average pore diameter.

attributed to a ''dilution'' effect caused by the presence of the supported cobalt oxide phase [16]. However, these authors estimated that the relative loss of surface area due to the ''dilution'' is about 20% for Co/ITQ-6 and Co/MCM-41 catalysts with 20 wt% of Co loading. The surface area and pore volume values reported in Table 1 clearly indicate that a partial plugging of the pores takes place. Therefore, it can be concluded that Co is partially located inside the channels.

The XPS analysis of the calcined samples indicates that no residual chlorine has been detected upon calcination at 400 °C. The Co 2p spectrum of the calcined catalysts shows the characteristic pattern of oxidic cobalt, with the Co $2p_{3/2}$ peak at 780.2–780.3 eV and a weak shake-up feature at higher binding energy. This binding energy is in good agreement with the binding energies reported in the literature for CoO/Co_3O_4 [17,18]. The existence of a weak shake-up feature indicates the formation of Co_3O_4 rather than CoO.

The average diameter of the supported cobalt particles in oxidized catalysts was investigated by HRTEM. As an example, Fig. 3 displays a TEM image of Co10/MCM-22[200]. TEM images indicate that Co nanoparticles with an average particle size of 6–7 nm are obtained for the Co catalysts supported on MCM-22 zeolites with a 10 wt% Co loading. The average size seems to be slightly decreased as the Co loading decreases. The average particle size in the reference Co/SiO_2 catalyst is shifted to higher values. Moreover, the distribution of cobalt particles seems to be more heterogeneous in Co/SiO_2.

The FTS catalytic performance of the different Co-supported catalysts was evaluated in a fixed-bed reactor at 280 °C, $H_2/CO = 2$, $P = 12.5$ bar. The syngas was diluted with He, He/syngas ratio = 5. These reaction conditions were chosen in order to favor the formation of relatively light products rather than waxes. The activity and selectivity data corresponding to the pseudo-stationary period (after stabilization on stream) are summarized in Table 2. The CO conversion is not significantly different for the Co catalysts with 10 wt% of Co. As expected, the CO conversion decreases as the Co loading is decreased. In all cases, a relatively low CO_2 formation is observed, clearly indicating a very low water gas-shift activity. However, this WGS activity seems to be even lower when the Co particles are supported on MCM-22 samples.

Table 2 indicates that the hydrocarbon selectivity depends on the properties of the support. As expected, the highest methane selectivity was obtained for sample Co10/MCM-22[45], in which the Na cations were partially exchanged by H^+. Obviously, this results in an increase of acidity, significantly increasing the cracking activity. Therefore, the C_{5+} selectivity is strongly decreased and the products are essentially restricted to the C_1–C_7 range. As the Si/Al ratio increases, the methane selectivity is decreased, while the C_{5+} selectivity is increased. Furthermore, the sample with the highest Si/Al ratio exhibits a slightly lower C_1 selectivity as compared to the conventional Co/SiO_2 catalyst. Although it has been reported that the C_1 selectivity is usually increased as the Co particle size decreased [5], this effect has not been observed on MCM-22-supported catalysts. Also, this catalyst shows a higher selectivity to C_{5+}. It is well known that FTS selectivity depends on the conversion level and one would expect an increase of C_{5+} selectivity with increasing the CO conversion. However, the C_{5+} selectivity values obtained for the Co catalyst supported on MCM-22[200] with different Co loadings seem to be independent of the conversion level. The chain growth probability during FTS

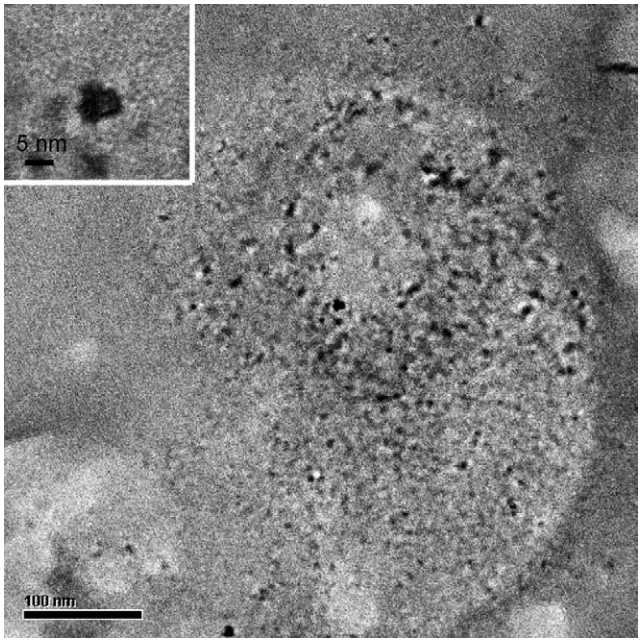

Fig. 3. Transmission electron micrographs of the cobalt-loaded MCM-22[200]. The inset indicates a ~7 nm cobalt particle.

Table 2
Catalytic results for the Fischer–Tropsch synthesis on Co catalysts

Sample	X (%)	S_{CO_2} (%)	Hydrocarbon distribution (wt%)				
			C_1	C_2–C_4	C_2/C_3	C_{5+}	C_5–C_9
Co10/MCM-22[45]	18.3	<0.1	40.4	41.4	0.96	18.2	18.2
Co10/MCM-22[90]	16.3	<0.1	28.3	45.6	1.28	24.5	19.9
Co10/MCM-22[200]	21.7	0.65	21.2	37.6	0.69	40.2	35.8
Co5/MCM-22[200]	9.7	0.30	23.8	39.7	0.72	35.9	32.9
Co2/MCM-22[200]	4.5	<0.1	20.3	36.9	0.70	42.2	35.4
Co10/SiO_2	14.3	2.1	23.8	51.7	1.15	24.7	21.9

and, therefore, the formation of longer hydrocarbon chains, on supported cobalt catalysts generally increases with the size of the reduced Co particles [10,19,20]. However, the increased C_{5+} selectivity observed over Co/MCM-22[200] as compared to Co/SiO_2 cannot be explained by an increase of the Co particles size. Then, the C_{5+} selectivity increase should be ascribed to the particular properties/structure of the Co particles supported on the MCM-22 material. Interesting, while the C_5–C_9 fraction increases significantly for the MCM-22[200] catalysts as compared to the silica-supported one, the C_{10+} fraction is not largely different.

4. Conclusions

In this contribution, we have applied silica-rich MCM-22 molecular sieves as supports for preparing cobalt-based Fischer–Tropsch catalysts. According to TEM measurements, Co/MCM-22 contained smaller and more uniform Co nanocluster than Co/SiO_2 catalyst. Moreover, the catalysts based on MCM-22 exhibited the highest selectivity to long-chain (C_{5+}) hydrocarbons upon utilizing MCM-22 supports with the appropriate Si/Al ratio. The higher C_{5+} selectivity could be attributed to particular properties of the Co particles. This might indicate that the structure of the MCM-22 zeolite played an important role in determining and controlling the selectivity in FTS.

Acknowledgments

This research was conducted under the auspices of A*Star, The Agency for Science, Technology and Research (Singapore), with the financial support of the Institute of Chemical and Engineering Sciences (ICES), Singapore.

References

[1] M.E. Dry, Catal. Today 71 (2002) 227.
[2] A.C. Vosloo, Fuel Process. Technol. 71 (2001) 149.
[3] P.J. Van Berge, S. Barradas, J. Van de Loodsrecht, J.L. Visage, Petrochemie 117 (2001) 138.
[4] T.H. Fleisch, R.A. Sills, M.D. Briscoe, J. Nat. Gas Chem. 11 (2002) 1.
[5] A.Y. Khodakov, A. Griboval-Constant, R. Bechara, V.L. Zholobenko, J. Catal. 206 (2002) 230.
[6] E. Dry, Appl. Catal. 276 (2004) 1.
[7] Y. Ohtsuka, Y. Takahashi, M. Noguchi, T. Arai, S. Takasaki, N. Tsubouchi, Y. Wang, Catal. Today 89 (2004) 419.
[8] M.E. Leonowicz, J.A. Lowton, S.L. Lawton, M.K. Rubin, Science 264 (1994) 1910.
[9] S.L. Lawton, M.E. Leonowicz, R.D. Partidge, P. Chu, M.K. Rubin, Microporous Mesoporous Mater. 23 (1998) 109.
[10] F.G. Botes, W. Böhringer, Appl. Catal. A 267 (2004) 217.
[11] E. Dumitriu, D. Meloni, R. Monaci, V. Solinas, C. R. Chim. 8 (2005) 441.
[12] A. Corma, V. Fornes, S.B. Pergher, Th.L.M. Maesen, J.G. Buglass, Nature 396 (1998) 353.
[13] A. Corma, V. Fornes, J. Martinez-Triguero, S.B. Pergher, J. Catal. 186 (1999) 57.
[14] M. Cheng, D. Tan, X. Liu, X. Han, X. Bao, L. Lin, Microporous Mesoporous Mater. 42 (2001) 307.
[15] A.M. Saib, M. Claeys, E. van Steen, Catal. Today 71 (2002) 395.
[16] P. Concepción, C. López, A. Martínez, V.F. Puntes, J. Catal. 228 (2004) 321.
[17] Z. Zsoldos, L. Guczi, J. Phys. Chem. 96 (1992) 9393.
[18] A.M. Hilmen, D. Schanke, K.F. Hanssen, A. Holmen, Appl. Catal. A 186 (1999) 169.
[19] R.C. Reuel, C.H. Bartholomew, J. Catal. 85 (1984) 78.
[20] A.Y. Khodakov, A. Griboval-Constant, R. Bechara, F. Villain, J. Phys. Chem. B 105 (2001) 9805.